CHIMIA 52 (1998) Nr. 10 (Oktober)

Chimia 52 (1998) 607–612

ISSN 0009–4293

The Melting Point of Crystalline Copolymers – Applying Materials Simulation

Jürgen Wendling and **Ulrich W. Suter***

Abstract. The defect *Gibbs* energy of hydroxyvalerate comonomer inclusions into the crystals made up by random copolymers of poly(β-hydroxybutyrate-*co*-β-hydroxyvalerate) (PHB/HV) is calculated by means of the thermodynamic integration approach. The result obtained for a single inclusion is in excellent agreement with those obtained by fitting experimental melting temperature and cocrystal composition data. On decomposing the *Gibbs* energy, it is found that the crystallization entropy contributes the dominant part of the defect *Gibbs* energy. Our calculations on multi-inclusion crystals show that the *Gibbs* energy strongly decreases when the comonomers aggregate in a preferred pattern. Further information to the design of isomorphic copolymers is obtained from these calculations.

Introduction

Random copolymers are widely used in materials development to tune their properties, such as the melting temperature or the convenient processing temperature. Introducing, *e.g.*, some ethylene or methylene units randomly into isotactic poly(propylene) (i-PP) promotes the formation of shorter, stereoregular blocks (of length ξ) and results in a linear depression of the melting point by almost 5 K per wt.-% of the comonomer [1]. Higher amounts of random comonomer inclusions reduce the probability of homopolymer sequences long enough to crystallize sufficiently that the material is obtained completely amorphous (*Fig. 1*).

The thermodynamic theory of crystallization of this type of copolymers, where the guest comonomers are excluded from the crystallization of the host polymer, was first discussed by *Flory* [2] and later augmented by *Baur* by a more phenomenologic theory [3][4] that fits the experimental data better than the *Flory* model.

A different type of crystallization is observed for some copolymers where the comonomers can be included into the crystal of the host polymer. Depending on the amount of comonomer included, the melting temperature is also reduced (albeit less than for the exclusion case), and crystallization may occur for the whole range of copolymer composition. The limit of uniform inclusion, where the concentration of the comonomer in the crystal is the same as in the entire copolymer, is displayed in *Fig. 2*.

Up to now, the crystallization of random copolymers of this type is not well understood. Theoretical models dealing with cocrystallization of random copolymers usually assume a random distribution of the comonomers in the crystal [5–7]. However, this assumption holds only for the idealized case where the defect is small enough as not to affect the arrangement of neighboring chains. In general, every defect (inclusion of a 'wrong' monomeric unit) creates available volume in the neighboring part of the crystal, making additional inclusions at these positions more likely then elsewhere. The deformation of the neighboring chains may be small and compensated by small rearrangements of the polymer chains in the surrounding of the defect without affecting the long-range order of the crystal when the two comonomers consist of constitutionally identical units with different configuration (*e.g.*, i/a-PP) or of units different only in the length of a flexible side chain (*e.g.*, i-PP/but-1-ene or poly(β-hydroxybutyrate-*co*-β-hydroxyvalerate (PHB/HV)).

The misfit created in chains of non-flexible units of rigid main-chain polymers by units of different length much stronger affects the crystal conformation and crystallization *Gibbs* energy, because it can not be compensated for within a small and localized region of the crystal. A popular example for rigid main-chain random copolymers is poly(hydroxybenzoic acid-*co*-hydroxynaphthoic acid) [8]. This

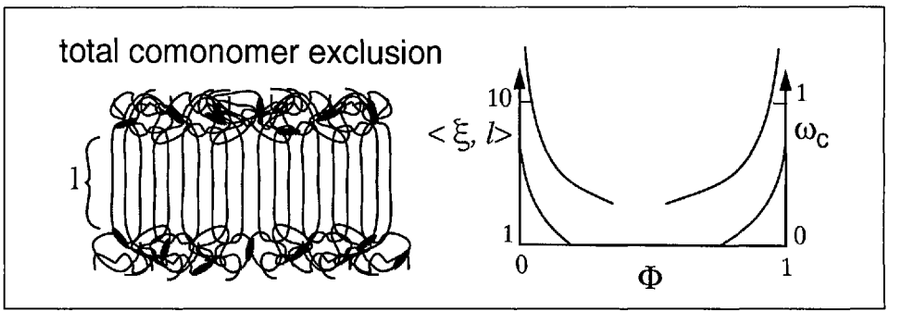

Fig. 1. *The exclusion crystallization of random copolymers.* Increasing amount of comonomers reduces the average homopolymer sequence length ξ and lamellar thickness, resulting in a strongly decreased degree of crystallinity ω_c.

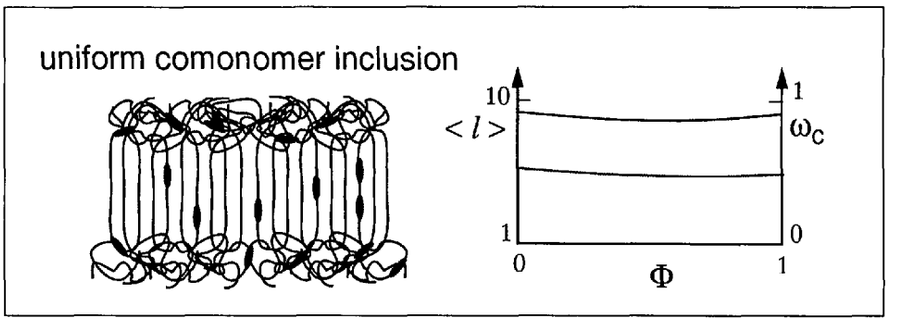

Fig. 2. *The uniform inclusion crystallization of random copolymers.* The comonomers take part in crystallization, and the morphology remains almost unchanged.

*Correspondence: Prof. U.W. Suter
Department of Materials
Institute of Polymers
Universitätstrasse 6, CNB E91.2
ETH-Zürich
CH-8092 Zürich

copolymer does not crystallize, but exists in the nematic liquid-crystalline state. However, crystallization of these copolymers is conceivable when the chains arrange by selection of similar and matching, yet random segments of the chain [9]. The probability of finding those matches is not too small, but it is uncertain whether these aggregates can reach the minimum size of thermodynamically stable crystal nuclei. The high molecular rigidity also might be limiting the chain mobility required for the constitutional matching of sequences.

In the first part of this paper, we discuss the theoretical background of copolymer crystallization and apply the crystallization model to experimental data. Here, the crystallization will be discussed in terms of the defect *Gibbs* energy, which is the energy required to replace one repeat unit in the crystal by a comonomer unit. The second part presents atomistic force-field simulations that gain more informations on the thermodynamics and conformation of the cocrystallization of random copolymers.

Thermodynamics of Copolymer Crystallization

The kinetic and equilibrium aspects of copolymer crystallization have been addressed by a number of authors [2–7]. The idea behind using equilibrium thermodynamic is based on the assumption that, considering a copolymer of two comonomers A and B crystallizing in the crystal lattice of A, the comonomers B may either be excluded from the crystals or act as defects in the crystal. In both cases, the *Gibbs* energy of the crystal will increase and the melting temperature decrease. In the following, we address exclusively random copolymers, *i.e.*, copolymers with a *Bernoulli*an distribution of monomer sequences.

The case of comonomer exclusion in thermodynamic equilibrium was first described by *Flory* [2], who calculated the upper bound of the copolymer melting temperature, *i.e.*, the melting temperature of crystals built up from 'infinitely long' homopolymer sequences of units A in the copolymer. *Flory* found the melting temperature *equation*:

$$\frac{1}{T_m^\circ} - \frac{1}{T_m(X_B)} = \frac{R}{H_m^\circ} \cdot \ln(1 - X_B) \quad (1)$$

X_B is the concentration of B units in the polymer and $\ln(1 - X_B)$ equals the collective activities of A sequences in the limit of the upper bound of the melting temperature. T_m° and H_m° denote the homopolymer equilibrium melting temperature and heat of fusion, respectively, and R is the gas constant.

The probability of finding those crystals is very low, leading *Kilian* [3] and *Baur* [4] to develop a phenomenologic theory of copolymer crystallization based on the behavior of eutectic mixtures. The basic idea is that the homopolymer sequences of length ξ may only be included into crystals of lamellar thickness corresponding to that length. The melting temperature is then given by

$$\frac{1}{T_m^\circ} - \frac{1}{T_m(X_B)} = \frac{R}{H_m^\circ} \cdot [\ln(1 - X_B) - \langle\xi\rangle^{-1}] \quad (2)$$

where $\langle\xi\rangle = [2 \cdot X_B(1 - X_B)]^{-1}$ is the average length of homopolymer sequences in the melt [4]. This model, while incorporating finite crystal thickness and the concomitant depression in the melting point, still neglects that the homopolymer sequences are invariably fixed in chains due to bond connectivity; the eutectic equilibrium, which requires total separation into the 'components' (the homopolymer sequences of same length ξ), is unrealistic. However, it was shown by several investigations [4][10] that the *Baur* model (*Eqn. 2*) fits experimental data much better than the *Flory* equation (*Eqn. 1*) [2].

Inspection of experimental data shows readily that comonomer exclusion alone cannot account for the observed melting-point depression in many cases. In *Fig. 3*, we plot the experimental excess crystallization *Gibbs* energy (obtained as $H_m^\circ/RT_m \cdot (1 - T_m/T_m^\circ)$) together with the corresponding theoretical values (calculated as $\ln(1 - X_B) - \langle\xi\rangle^{-1}$ in case of the *Baur* model) as a function of copolymer composition. In case of PEN/T and PHB/HV copolymers, the experiment and *Baur* model match the data at low comonomer composition, indicating that the comonomer exclusion model may hold in this range of composition. However, beyond a certain composition, the experimental excess *Gibbs* energy is lower for these copolymers, and for copolymers of i-PP, experimental values are always lower than those obtained by the model. Exclusion theories do not account for these observations,

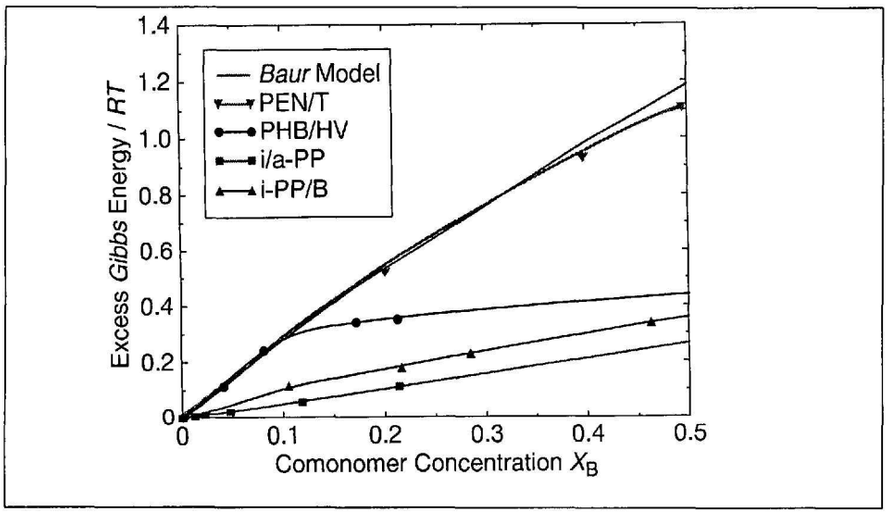

Fig. 3. *Excess* Gibbs *energy/*RT *as obtained from experiment for random copolymers of PEN/T (poly(ethylene 2,6-dicarboxynaphthanoate-*co*-terephthalate))* [18], *PHB/HV (poly(*β*-hydroxybutyrate-*co*-*β*-hydroxyvalerate)* [11], *i/a-PP (stereoregularity defect in isotactic poly(propylene))* [19], *and i-PP/butene-1 (isotactic poly(propylene-*co*-butene-1))* [20], *compared to the theoretical value given by* Baur*'s copolymer exclusion theory* [4]

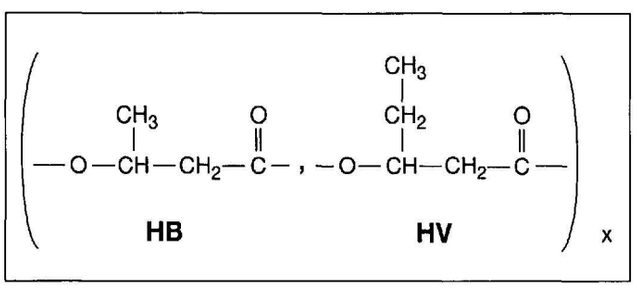

Fig. 4. *The PHB/HV copolymer*

hence, comonomer inclusion is to be considered in melting-point prediction.

At least, one additional parameter, the defect *Gibbs* energy of a comonomer inclusion, is required for models dealing with comonomer inclusions. Models that consider the possibility of comonomer inclusions were first discussed by *Helfand* and *Lauritzen* [5] and by *Sanchez* and *Eby* [6]. They assumed that the defects are randomly distributed in the crystal and do not interact with each other, so that they could be described by a mean defect *Gibbs* energy ε ($\varepsilon \geq 0$).

Sanchez and *Eby* found that the melting temperature can be described by:

$$\frac{1}{T_m(X_B)} - \frac{1}{T_m^\circ} = \frac{R}{H_m^\circ} \cdot \left\{ \frac{\varepsilon \cdot X_{CB}}{RT_m} + (1 - X_{CB}) \cdot \ln \frac{1 - X_{CB}}{1 - X_B} + X_{CB} \cdot \ln \frac{X_{CB}}{X_B} \right\} \quad (3)$$

X_B is the overall concentration of B in the melt and X_{CB} the actual concentration of B in the cocrystal that is largely determined by the kinetic conditions of the crystal formation. ε (X_{CB}) is the average defect *Gibbs* energy required to replace one repeat unit in the crystal by a comonomer and depends, in general, on the concentration of included comonomers, $\varepsilon = \varepsilon(X_{CB})$.

The behavior at $\varepsilon \gg 0$ is the principal shortcoming of the *Sanchez-Eby* model: when ε is too high to allow cocrystallization, *Eqn. 3* reduces to *Eqn. 1* of the *Flory* model, but it should preferentially converge to the *Baur* model, *Eqn. 2*. We achieved a more general melting-temperature equation for copolymers in a frustrated thermodynamic equilibrium following the derivations of *Flory* [2], *Baur* [4], and *Sanchez* and *Eby* [6]. Without going into details that are described elsewhere [7], the melting temperature is now given as:

$$\frac{1}{T_m(X_B)} - \frac{1}{T_m^\circ} = \frac{R}{H_m^\circ} \cdot \left\{ \frac{\varepsilon \cdot X_{CB}}{RT_m} + (1 - X_{CB}) \cdot \ln \frac{1 - X_{CB}}{1 - X_B} + X_{CB} \cdot \ln \frac{X_{CB}}{X_B} + \langle \tilde{\xi} \rangle^{-1} \right\}$$

(new model) (4)

where $\langle \tilde{\xi} \rangle^{-1}$ is found in analogy to *Baur*'s approximation, treating the fraction X_{CB} of B units that are cocrystallizing as if they were units of A, as

$$\langle \tilde{\xi} \rangle^{-1} = 2 \cdot (X_B - \tilde{X}_{CB}) \cdot (1 - X_B + \tilde{X}_{CB}) \quad \text{for } \tilde{X}_{CN} \leq X_{CB} \text{ and 0 else} \quad (5)$$

where $\tilde{X}_{CB} = X_{CB} \cdot (1 - X_B)/(1 - X_{CB})$ is the concentration of B units (with respect to the entire copolymer) that are included into the crystal. Notice that the concentration X_{CB} is related to the crystal only.

Assuming equilibrium comonomer inclusion, where X_{CB} is given by the *Boltzmann* weight of ε, *Eqn. 4* reduces to

$$\frac{1}{T_m^\circ} - \frac{1}{T_m(X_B)} = \frac{R}{H_m^\circ} \cdot \{ \ln(1 - X_B) + X_B \cdot e^{-\varepsilon/RT} - \langle \tilde{\xi} \rangle^{-1} \} \quad \text{(new model, equilibrium)} \quad (6)$$

with

$$\langle \tilde{\xi} \rangle^{-1} = 2 \, (X_B - X_B \cdot e^{-\varepsilon/RT}) \, (1 - X_B + X_B \cdot e^{-\varepsilon/RT}) \quad (7)$$

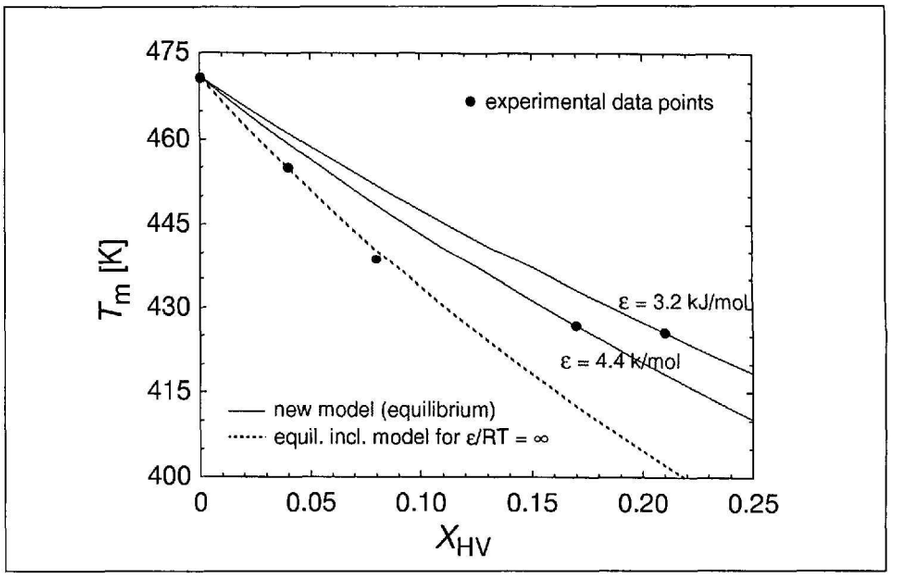

Fig. 5. *Experimental equilibrium melting temperatures* T°_m *vs. copolymer composition.* The lines display the expected melting temperatures depending on the cocrystallization model (see text). The data points are taken from *Orts*, *Marchessault*, and *Bluhm* [11].

Comparison to Experimental Data

We tested our model on several copolymers, but we will focus here on the random copolymer of poly(β-hydroxybutyrate-co-β-hydroxyvalerate), PHB/HV (*Fig. 4*).

A set of experimental data for the equilibrium melting temperature of PHB/HV copolymers was recently published by *Orts*, *Marchessault*, and *Bluhm* [11]. The authors crystallized copolymers at different melting temperatures and extrapolated their data for T_m with inverse lamellar thickness to infinite lamellar (crystal) size. The so-obtained equilibrium melting temperatures T_m° are plotted in *Fig. 5*. The crystal HV concentration X_{CV} was determined by *VanderHart*, *Orts*, *Marchessault*, and *Bluhm* by means of solid-state ^{13}C-NMR spectroscopy [12] and small-angle X-ray scattering [13]. Both investigations revealed that the amount of HV units that are included into the HB crystal increases with increasing HV concentration in the copolymer.

These melting temperatures and crystal composition data are used to calculate an experimental estimate of the defect *Gibbs* energy based on the different models described above. An illustration of

these models for the PHB/HV copolymer is already given in *Fig. 5*. The dashed line corresponds to the complete exclusion of comonomers due to a sufficiently high defect *Gibbs* energy (which is equal to the *Baur* model, *Eqn. 2*), whereas the thin lines correspond to the equilibrium inclusion model, *Eqn. 6*, using different estimates for the defect *Gibbs* energy. As the melting temperatures at HV concentrations of 0.17 and 0.21 exceed the prediction of the exclusion model, some cocrystallization must occur at these concentrations.

Table 1 gives the defect *Gibbs* energies obtained by the different models; the differences make clear that knowledge of the real crystal composition is of great importance. An estimate for $X_V = 0$ is obtained by linear extrapolation of the experimental data for X_{CB} towards zero concentration which yields $\langle\varepsilon\rangle = 17.8$ kJ/mol.

These models, however, give no insight on the detailed crystal morphology. To gain more information, force-field computer simulations were performed to calculate the defect *Gibbs* energy for single- and multi-inclusion copolymer crystals.

Simulation of Comonomer Inclusion *Gibbs* Energies

For the assessment of the inclusion of a single comonomer unit into a homopolymer crystal, the problem to be treated computationally is the transformation from a system at state $\lambda = 0$ (a homopolymer single crystal of the host polymer plus one individual chain with a comonomer unit, somewhere outside) into a system at state $\lambda = 1$ (a copolymer crystal that includes one 'defective' chain plus one host-homopolymer chain unit outside). This 'reaction' (*Fig. 6, a*) would be governed by the excess *Gibbs* energy ε, usually called the single inclusion defect *Gibbs* energy. The approach that is more convenient to molecular dynamics (MD) calculations is the thermodynamic integration approach that estimates only the energy difference of the two states by slowly transforming the system from state $\lambda = 0$ to $\lambda = 1$ (*Fig. 6, b*). Crystal and single co-unit are transformed independently, but the sum of both calculations gives the *Gibbs* energy difference corresponding to the exchange reaction. During the transformation that is described in detail in [14], the derivative of the systems *Hamiltonian* with respect to the state of transformation described by λ must be calculated and the transformation *Helmholtz* energy (in an *NVT* ensemble) is then obtained by integration as [15]:

$$\Delta A_{0\to1} = \int_0^1 \left\langle \frac{\partial H(\lambda)}{\partial \lambda} \right\rangle_\lambda d\lambda \qquad (8)$$

For further analysis, the *Helmholtz* energy was divided into an enthalpic and an entropic contribution as follows: the internal energy of defect inclusion was calculated as the total energy difference between the defective and the defect-free microstructure, *i.e.*,

$$\Delta E_{0\to1} = \langle H(\lambda = 1)\rangle - \langle H(\lambda = 0)\rangle \qquad (9)$$

The values were taken from 50 ps *NVT*-MD calculations of the microstructures before and after the thermodynamic integration calculations were performed. The entropy change on defect inclusion is then given by

$$\Delta S_{0\to1} = (\Delta E_{0\to1} - \Delta A_{0\to1})/T \qquad (10)$$

As experimental results usually are obtained at constant pressure conditions, the calculated *Helmholtz* energy needs to be transformed into *Gibbs* energy for comparison. We approximate the *Gibbs* energy difference $\Delta G_{0\to1}$ by adding the mechanical work (approximated by the mean pressure-energy change $p\,\Delta V$) to $\Delta A_{0\to1}$ from the thermodynamic integration results.

For all discussions in this paper on the HB → HV transformation, a value of the coupling parameter $\lambda = 0$ corresponds to the HB structure of the repeat unit under transformation, whereas a value of $\lambda = 1$ corresponds to the HV structure. We consider the configuration at $\lambda = 0$ as the starting point of the thermodynamic integration and the configuration at $\lambda = 1$ as the finishing point.

Gibbs *Energy of Single Comonomer Inclusion*

A PHB/HV microstructure is shown in *Fig. 7*. One HB repeat unit is already replaced by a HV unit and labelled with

Table 1. *Values of the Average Defect* Gibbs *Energy* <ε>: Calculated from experimental melting temperature and cocrystal composition data, compared to those obtained from the uniform inclusion and equilibrium inclusion models.

Experimental values [11–13]			Average defect *Gibbs* energy [kJ/mol]		
X_B	X_{CB}	T_m [K]	non-equil. inclusion, X_{CB} from exp.	uniform inclusion, $X_{CB} = X_B$	equilibrium inclusion $X_{CB} = X_{CB}^{(eq)}$
0.04	0.016	455	14.9	11.1	∞
0.08	0.023	439	15.9	11.2	∞
0.17	0.097	427	6.4	7.2	4.4
0.21	0.119	426	4.2	6.0	3.2

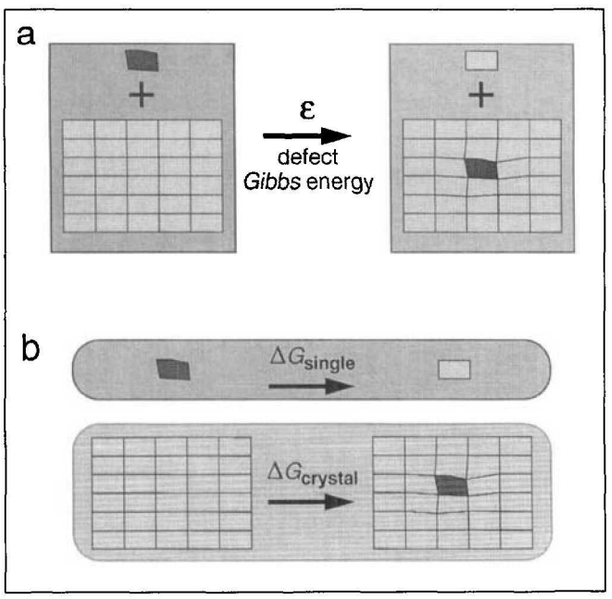

Fig. 6. *Concept of the defect inclusion procedure. a*) The direct exchange of one host-polymer repeat unit by one guest unit; this exchange is characterized by the defect *Gibbs* energy ε. *b*) The computational treatment of this exchange where the crystal and the single unit are transformed independently.

CHIMIA 52 (1998) Nr. 10 (Oktober)

'1'. We transformed this unit to HV by thermodynamic integration.

The integration utilizing the trapezoidal integration scheme is illustrated in *Fig. 8*, and the integration results are listed in the first line of *Table 2*. After correcting for the mean mechanical work, the *Gibbs* energy difference between the defect creation in the PHB crystal and the PHB chain is found to be 16.5 kJ/mol, which is quite close to the estimate from experiments given in the previous section of this paper and within the range of uncertainty of these estimates. The further analysis of our data makes clear that this *Gibbs* energy difference is dominated by the conformational entropy; investigating cocrystallization by calculating the defect energy ΔE only would suggest, if available as the only piece of information, the misleading interpretation that cocrystallization is thermodynamically favored as soon as the assumption of independent defects is given up. The data for $T\Delta S$ given in *Table 2* demonstrate that indeed the crystallization entropy dominates the *Gibbs* energy of comonomer inclusion and that its influence may not be neglected.

Defect Aggregation

In order to evaluate possible interactions between defects, the *Gibbs* energy calculations were now extended analogously to several defects in a microstructure. In particular, we focused on the question in how far the aggregation of HV units could lower the mean defect *Gibbs* energy.

A second HV defect was incorporated close to the first one (defect concentration of 1.5%); since there are two crystallographically distinct monomeric units in the unit cell, both of these positions were tested with the next unit cell in each of the principal cell directions.

The selected positions for this additional HV units are labelled in *Fig. 7*: The defects 'a_1', 'a_2', 'b_1', 'b_2' are located in the (h k 0) plane of the microstructure (taking the position of '1' as (0 0 0), see *Table 2* for exact positions), whereas defects 'c_1' and 'c_2' are the next and the following possible positions in the same chain as defect '1'. *Gibbs* energies for these defects are listed in *Table 2*. All features of the simulation of single defects, described above, apply also to the structures with two defects. It is obvious that the HV units at positions 'a_1', 'b_1', and 'c_1' produce a defect *Gibbs* energy similar to the energy of the first HV inclusion, whereas the units at positions 'a_2', 'b_2', and 'c_2' give an average defect *Gibbs* energy that is on average 13% lower.

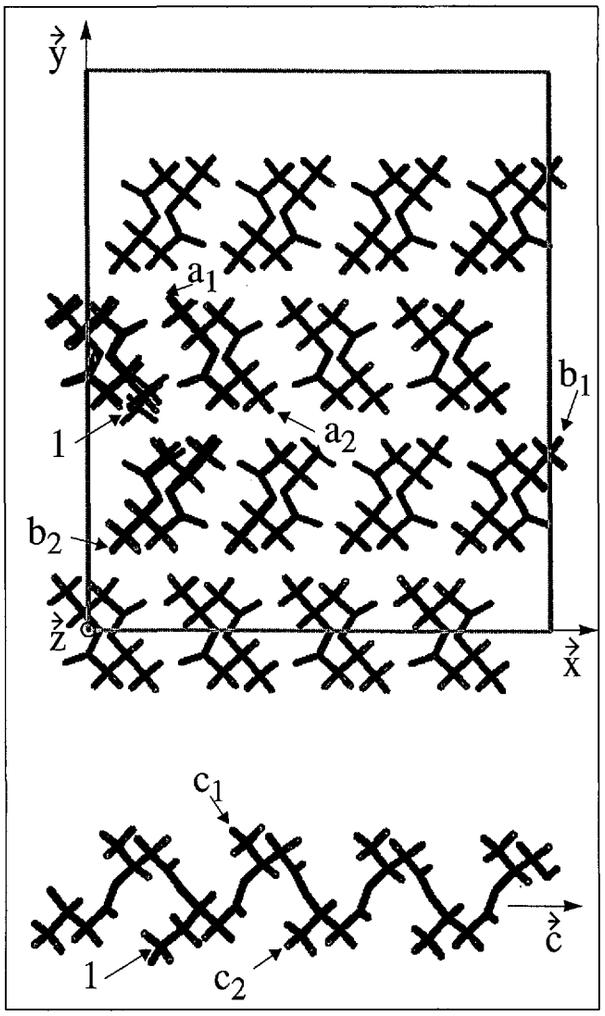

Fig. 7. *Sketch of the PHB microstructure.* This box contains 16 chains with 8 repeat units each (32 crystallographic unit cells). One HV repeat unit is incorporated and labelled with '1'. Other labels indicate the positions where further defects will be created: the defects 'a_1', 'a_2', 'b_1', and 'b_2' are located in the (h k 0) plane of the microstructure (taking the position of '1' as (0 0 0)), whereas defects 'c_1' and 'c_2' are located at (0 0 1/2) and (0 0 1), respectively.

This is in contrast to investigations of *Kamiya et al.* [16] who surmised decreasing average defect *Gibbs* energies when diads HV–HV are included into the crystal. Based on our calculations, triads of type HV–HB–HV would have to be responsible for the decrease of ε. This behavior may be explained by a simple argument: a defect included at one position deforms the surrounding crystal lattice. A second defect far away from the first has its own deformation domain and gives rise to a defect *Gibbs* energy similar to that of the first defect. A second defect very close to the first one (inside its deformation domain) faces a defective lattice to deform that contains the additional CH_3 group in its deformation domain and hence gives rise to a similar defect *Gibbs* energy than the first defect.

That is the case for the defects at positions 'a_1', 'b_1', and 'c_1' (see *Fig. 7*). However, if the second defect is located outside the deformation domain of the first one, but these domains overlap and cause displacements in the same direction, then the second defect benefits from the work of deformation done by the first one, leading to synergistic effects that lower the average defect *Gibbs* energy of this pair. This may explain the lower defect *Gibbs* energy at positions 'a_2', 'b_2', and 'c_2'. These defects are oriented similarly as '1' revealing similar orientations of the anisotropic deformations domains, whereas the other defects ('a_1', 'b_1', and 'c_1') produce deformation domains with different displacements.

Extension to Higher Comonomer Concentrations

Based on our *Gibbs* energy calculations, a stronger decrease of the average defect *Gibbs* energy seems possible when the number of aggregated HV units increases, enabling higher degrees of cocrystallization. Unfortunately, the large variety of possible aggregates makes *Gibbs* energy calculations based on the thermodynamic integration approach impossible. However, lattice calculations based on nearest-neighbor interactions might give a good estimate on the possible behavior. We chose a finite cubic lattice with *von*

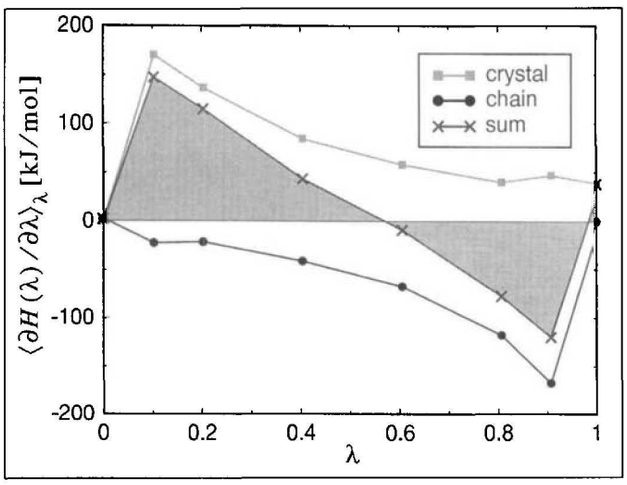

Fig. 8. *The thermodynamic integration result for a single HV inclusion in a PHB microstructure.* See also *Table 2.*

Table 2. *Values (per Defect) of the* Helmholtz *and* Gibbs *Energy Change Calculated for the Inclusion of One or Two* β*-Hydroxy-valerate Defects into a PHB Crystal at T = 300 K.* Defect *Gibbs* energy ΔG is obtained from *Helmholtz* energy ΔA after correcting for the mean mechanical work. The internal energy change ΔE is taken from *NVT* calculations before and after defect inclusion. The average numbers are calculated for the double inclusion results only. The statistical errors in the calculations of ΔA and ΔG are in the range of 1.6 kJ/mol.

Created Defect	Position of 2nd			ΔA	ΔG	ΔE	$T\Delta S$	ΔS
	Fractional coord.			[kJ/mol]	[kJ/mol]	[kJ/mol]	[kJ/mol]	[J/mol/K]
1	0	0	0	17.3	16.5	2.1	–15.2	–6.1 R
$(1 + a_1)$	0.33	0.3	0.52	16.9	16.3	7.1	–9.8	–3.9 R
$(1 + a_2)$	1	0	0	15.1	14.6	1.7	–13.3	–5.3 R
$(1 + b_1)$	–0.49	–0.2	–0.22	17.7	16.9	–5.8	–23.5	–9.4 R
$(1 + b_2)$	–0.16	–0.5	0.28	14.8	14.1	–8.2	–23.0	–9.2 R
$(1 + c_1)$	–0.66	0.30	0.5	17.4	16.9	3.9	–13.5	–5.4 R
$(1 + c_2)$	0	0	1	15.1	14.6	3.6	–11.5	–4.6 R

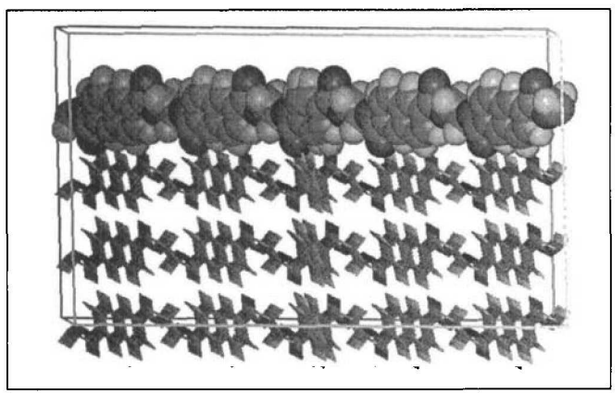

Fig. 9. *Simulation microstructure of a PEN/T crystal where the middle layer perpendicular to the image plane has already been transformed to ethylene terephthalate*

Neumann interactions. Hence, each lattice site has six interacting neighbors, two in each principal direction. Following the results of the thermodynamic integration approach for two defects, in our model, we only consider the interactions of a test lattice site with units on positions in the direction of the positive axes, (*i.e.*, 'a_2', 'b_2', and 'c_2'). Interactions to units in the other positions ('a_1', 'b_1', and 'c_1') are ignored because the changes of ε are smaller than the statistical errors of our *Gibbs* energy estimates.

This procedure leeds to an energy of 4.1 kJ/mol when all possible test sites around a comonomer are allocated by a comonomer; this corresponds to a 100% HV inclusion. This is already in the range of thermal energy and enables such aggregates to participate in crystallization.

The strength of these interaction effects can be illuminated more clearly on polymers crystallizing in an extended-chain conformation. One example are the copolymers of poly(ethylene 2,6-dicarboxynaphthanoate-*co*-ethylene terephthalate), PEN/T. Using our *Gibbs* energy calculation scheme, we found an inclusion *Gibbs* energy of 84 kJ/mol for a single inclusion [17], which reduces to 22 kJ/mol per comonomer when including an infinitely large layer in the *a-b* plane of the crystal (*Fig. 9*, the chains are extended in the *c*-direction). This results supports the non-periodic layer model that is preferred for the crystallization of non-flexible copolymers [18].

We gratefully acknowledge financial support from *DSM* and *Akzo Nobel* (The Netherlands) and for *J.W.* from the *Deutsche Forschungsgemeinschaft* (Grant No. DFG We 2134/1-1). We also appreciate stimulating discussions with *Peter Neuenschwander*, *Birgitta Nick*, and *Serge Santos* of the Department of Materials at ETH.

Received: July 20, 1998

[1] J. Karger-Kocsis, Ed., 'Polypropylene. Structure, blends and composites', Vol. 2: 'Copolymers and Blends', Chapman & Hall, London, 1995.
[2] P. L. Flory, *Trans. Faraday Soc.* **1955**, *51*, 848.
[3] H.G. Kilian, *Kolloid-Z. Z. Polymere* **1965**, *202*, 97.
[4] V.H. Baur, *Makromol. Chem.* **1966**, *98*, 297.
[5] E. Helfand, J.I. Lauritzen, *Macromolecules* **1973**, *6*, 631.
[6] I.C. Sanchez, R.K. Eby, *Macromolecules* **1975**, *8*, 638.
[7] J. Wendling, U.W. Suter, *Macromolecules* **1998**, *31*, 2516.
[8] A. Biswas, J. Blackwell, *Macromolecules* **1988**, *21*, 3146 ff.
[9] S. Hanna, A.H. Windle, *Polymer* **1988**, *29*, 207; S. Hanna, A.Romo-Ruibe, A.H. Windle, *Nature (Lomdon)* **1993**, *366*, 546.
[10] N. Yoshie, Y. Inoue, H.Y. You, N. Okui, *Polymer* **1994**, *35*, 1931.
[11] W.J. Orts, R.H. Marchessault, T.L. Bluhm, *Macromolecules* **1991**, *24*, 6435.
[12] D.L. VanderHart, W. J. Orts, R.H. Marchessault, *Macromolecules* **1995**, *28*, 6394.
[13] W. J. Orts, D.L. VanderHart, T.L. Bluhm, R.H. Marchessault, *Can. J. Chem.* **1995**, *73*, 2094.
[14] J. Wendling, U.W. Suter, submitted for publication.
[15] P.M. Allen, D.J. Tildesley, 'Computer Simulations of Liquids', Oxford, 1987.
[16] N. Kamiya, M. Sakurai, Y. Inoue, R. Chujo, *Macromolecules* **1991**, *24*, 3888.
[17] J. Wendling, A.A. Gusev, U.W. Suter, *Macromolecules* **1998**, *31*, 2509.
[18] X. Lu, A.H. Windle, *Polymer* **1995**, *36*, 451.
[19] S.Z.D. Cheng, J. J. Janimak, A, Zhang, E.T. Hsieh, *Polymer* **1991**, *32*, 648.
[20] P. Cavallo, E. Martusecelli, M. Pracella, *Polymer* **1977**, *18*, 42.